2020년 2월
석사학위 논문

친환경 젤 추진제의 전기 분해 및 점화

조선대학교 대학원
항 공 우 주 공 학 과
김 명 진

친환경 젤 추진제의 전기 분해 및 점화

Electrolytic decomposition and
ignition of green gelled propellant

2020년 2월 25일

조선대학교 대학원

항 공 우 주 공 학 과

김 명 진

Electrolytic decomposition and ignition of green gelled propellant

지도교수 김 태 규

이 논문을 공학 석사학위신청 논문으로 제출함

2019년 12월

조선대학교 대학원

항 공 우 주 공 학 과

김 명 진

김명진의 석사학위논문을 인준함

위원장 조선대학교 교 수 이 현 재 (인)

위 원 조선대학교 교 수 김 태 규 (인)

위 원 조선대학교 교 수 이 창 열 (인)

2019년 11월

조선대학교 대학원

Content

ABSTRACT

친환경 젤 추진제의 전기 분해 및 점화

Kim, Myoungjin
Advisor : Prof. Kim, Taegyu, Ph.D.
Department of Aerospace Engineering
Graduate School of Chosun University

우주 개발의 핵심은 엔진의 개발이라 할 수 있다. 과거 대형 발사체 위주의 연구가 주로 수행 되었다면 최근에는 큐브 위성의 개발과 관련하여 추력기의 소형화에 관한 연구가 많이 수행되고 있다. 현재 가장 많이 사용되는 하이드라진 추력기는 ~220 sec 수준의 비추력 특성을 가지고 있으며 많은 위성 시스템의 자세제어 추력기로 사용된 바가 있다. 그러나 이들의 높은 독성은 환경 문제 및 취급 문제로 인해 이를 대체하고자 하는 움직임이 활발하다. 과산화수소가 대체 후보군에 있으나 비추력이 낮은 특성을 가지고 있다. 이에 대해 새로운 추진제 합성 및 젤 추진제 적용이 제안 되었다. '친환경 추진제'라 불리는 ADN과 HAN 등 추진제는 특별한 보호 장구 없이 취급이 가능하며 생성물 또한 수증기가 다수를 차지한다. 젤 추진제의 경우 독성 추진제를 기반으로 하며 적절한 첨가제를 통해 증기압을 낮추고, 첨가제의 종류에 따라 비추력 특성을 증가시킬 수 있는 장점이 있다. 그러나 이원 추진제의 연료로 사용되는 하이드라진 단일 추진제의 경우 젤 추진제는 오히려 비추력을 낮출 수 있는 단점을 가지고 있다. 반면 ADN과 HAN은 각각 27%, 33%의 높은 산소 균형(Oxygen balance)을 가지고 있어 산화제로 작용하며 적절한 젤 화제 첨가는 연료로 작용하여 예혼합 단일 추진제로 사용이 가능하다. 그러나 이들의 가장 큰 문제는 점화에 어려움이 있다는 점이다. 분해 시 발생하는 고온의 가스는 장기적으로 활성 촉매 손실로 인한 연소 효율 감소 및 지속적인 고온 고압의 환경에 노출된 촉매 지지체의 구조적 불안정성은 이들의 우주 추진제 적용에 큰 장애물로 작용한다. 이를 해결하기 위해 다양한 방법이 제시되었다. 본 연구에서는 ADN에 비해 상대적으로 합성이 용이한 HAN을 기반으로 하는 친환경 젤 추진제를 직접 합성하고 이온 특성을 갖는 HAN 추진제의 전기 점화를 통한 점화 특성에 대해 수행하였다. 실험 결과 기존에 비해 11% 수준의 전기에너지 소모를 통해 5 sec 수준의 점화 지연 시간을 얻을 수 있었다.

List of figure

Chapter. 1

Chapter. 3

List of table

Chapter. 1

Chapter. 2

Chapter 1. Introduction

1.1 Introduction to rocket propulsion

Since the first rocket engine had been launched in 1926, various types of rocket engine have been developed for launch vehicles, space exploration from moon to over the solar system, and military purposes. In contrast with air-breathing engines such as turbofan and turbojet engine, rocket can be operated in the space where no air is existed. The major difference is that the rocket engine stores the both oxidizer and fuel in the vehicle. Therefore, it can be operated in the space where the oxygen is not existed. The drive force of rocket, thrust, is produced by the energy conversion from a thermal energy which is generated as a result of propellants combustion in the combustion chamber to a kinetic energy which is generated as the product gases pass through the nozzle[1]. The classification of rocket engine is defined by the types of propellant phase, liquid rocket, solid rocket, and hybrid rocket.

First of all, a liquid rocket uses the both liquid phase oxidizer and fuel. Moreover, liquid rocket is classified into bipropellant and monopropellant, which is stored the propellant in two separate tank and in a single tank, respectively. A liquid bipropellant rocket has mainly been developed for a launch vehicle system, such as space shuttle and KSLV(Korea Space Launch Vehicle). The propellant combinations for bipropellant rockets are liquid oxygen(LOX)/liquid hydrogen(LH_2), LOX/Kerosene, and dinitrogen tetroxide(N_2O_4)/hydrazine(N_2H_4). The first two combinations are mostly employed in launch vehicles, and later one is used in satellite orbit transfer. Meanwhile, monopropellants have an advantage that it can produce enough high thrust and specific impulse(I_{sp}) in a limited space of satellite systems with a single propellant. Furthermore, monopropellants have been employed in RCS(Reaction Control System) and DACS(Divert Attitue Control Syetem) of launch vehicles[2]. Secondly, a solid rocket uses solid phase

propellant of which an oxidizer is entrapped in an energetic fuel binder. The advantages of solid rocket are that the long term storage and ready-to-fire are available. For those reasons, most solid rockets have been developed for military purpose, such as inter-continental ballistic missile(ICBM). Finally, a hybrid rocket uses liquid phase oxidizer and solid phase fuel. The major advantage is that the long term storage and throttling are available. However, the regression rate of solid fuel is lower, therefore the overall system volume is increased to meet the same or similar performance of a liquid rocket engine.

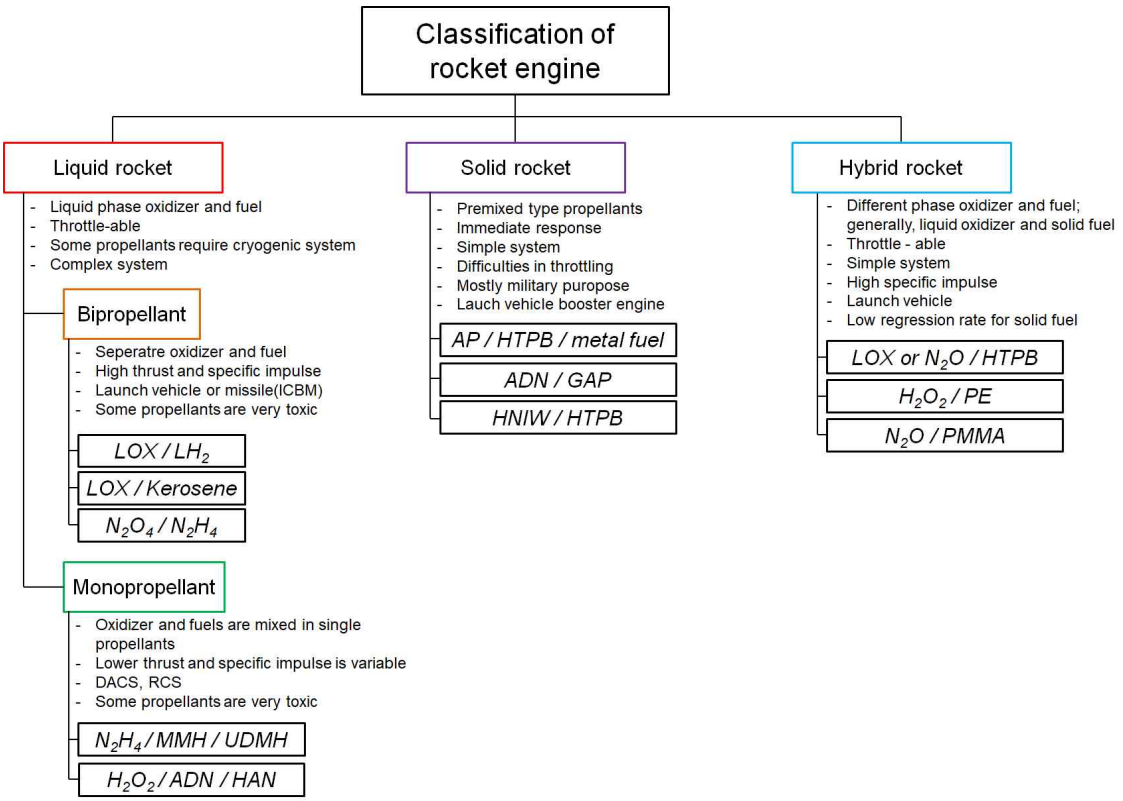

Fig. 1.1. Classification of rocket engine

Table 1.1 Some properties of rocket engines[1,3]

	Liquid rocket				Solid rocket	Hybrid rocket
	Bi propellant		Mono propellant			
Propellant	LOX/LH_2	LOX/ Kerosene	N_2H_4	H_2O_2	AP/HTPB/Al	N2O/PMMA
T_{ad}(K)	3000	3600	873	910	3300	3000
I_{sp}(sec)	300 ~ 420	290 ~ 320	200 ~ 220	140 ~ 190	260 ~ 280	~240
Application	SSME RS-25	KSLV Falcon	RCS Satellite DACS		Missiles (e.g. ICBM)	

1.2 Recent research issues

Recent research issues on rocket engineering can be categorized as shown below.

1) Liquid rocket
- Improved thermal management technology and increased thermal efficiency [4,5]
- Reuseable launch vehicle[6]
- Green hypergolic[7-10]
- Novel propellant synthesis that is non - toxic, easy to handle, and high (density)specific impulse[11-15]
- Ignition and combustion of novel monopropellants[13,14] (HAN and ADN based propellants)

2) Solid rocket
- Smokeless and/or flameless propellant[16]
- Chlorine(e.g. AP(NH_4ClO_4) replacement) free propellants[17,18]
- Thrust and combustion controllable propellants[19]
- Energetic thermoplastic propellants[20,21]

3) Hybrid rocket
- Nitrous oxide(N_2O) based rocket[22]
- Increased regression rate solid fuel[23]

In the case of a liquid rocket engine, the turbopump system and closed cycle engine to increase the energy efficiency are dominantly carried out as a part of KSLV development program. Internationally, a reuseable vehicle systems is researched to reduce the launch price. In addition, a hypergolic propellant survey is extensively studied. Conventional hypergolic propellants, such as hydrazine and

fuming nitric acid, are highly toxic to handle. However, a novel propellants called energetic ionic liquids which is mainly made up of dicyanamide are reported with lower toxicity and high hypergolic characteristics. Finally, a green propellant that can replace N_2H_4 and H_2O_2 monopropellant system is also extensively carried out. As the high toxicity of N_2H_4 which is employed for the satellite DACS propellant burdens the handling process, ADN(Ammonium dinitramide) and HAN(Hydroxylammonium nitrate) based novel green propellants are introduced from synthesis to flight test, such as LMP-103s and FLP-106 which are based on ADN, and SHP-163 and AFM-315E which are based on HAN. However, those green propellant are unfavorable with a previously developed catalysts and have some difficulties in the ignition sequence. In regard with replacement of toxic propellant issues, the gel propellants are also suggested, which increase the accessibility for handling the propellants as well as decrease the vapor pressure.

By considering the major application of the solid rocket, the stealth technologies which are smokeless and/or flameless are studied. As AP(Ammonium perchlorate) oxidizer and Al(Aluminum) nano metal fuel which are widely used in various solid rocket missiles form the smoke vigorously when the product gases reacts with vapor, a counter-detection becomes easier only by the eyes. Furthermore, a chlorine(-Cl) free propellant to reduce the environmental effects by the chlorine(Cl) components in AP which forms hydrochloric acid(HCl) vapor that devastates the ozone area is studied. In addition, the energetic thermoplastic propellants are also studied to increase the mixing process by applying the thermoplastic characteristic which is fluidic property as the temperature is increased. Finally, the electrically controllable propellants have been developed to overcome the conventional solid rocket drawbacks that the multiple ignition and extinguishing are impossible. The research scope in this research is focused on synthesis of novel monopropellant, HAN, and electrolytic ignition method. In addition, gelation process is conducted.

1.3 Conventional and novel monopropellants

Today, the most widely used monopropellant is N_2H_4 and its derivatives like UDMH(Unsymmetric dimethylhydrazine) and MMH(Mono methylhydrazine). The thruster which is developed by Aerojet-rocket dyne shown in Fig. 1.2 has been used for in-space flight at least 16,000 units[24]. In South Korea, Korea Aerospace Research Institute and HANHWA co. ltd. have developed 30 N and 200 N scale thruster[25]. One of the major advantages of N_2H_4 thruster is its high reliability. As the repair of satellite system, which operates in long term, is impossible, all equipped system must be established a high reliability. In this perspective, N_2H_4 thruster has a considerable advantage. Furthermore, its high reactivity makes the immediate responsible be available, which is critical factor for DACS. However, as shown in Fig. 1.3, a high level protection gear should be equipped when handling the N_2H_4 due to its a high toxicity. In addition, a spill and leakage to outside is lethal as dilution only by water is insufficient. One alternative candidate is H_2O_2(Hydrogen peroxide) of which the concentration for thruster usage is over 90% and either has a high reactivity like N_2H_4. As its toxicity is extremely lower than the N_2H_4, relatively light protection gear is enough to handle the H_2O_2. However, H_2O_2 has hypergolic property which would cause an unexpected explosion. Moreover, a high active oxygen loss rate is reported, and H_2O_2 thruster has lower I_{sp}. The application on H_2O_2 thruster is RCS of launch vehicle[26]. Despite of N_2H_4 and H_2O_2 have significant advantages such as high reliability and green nature, many researchers have been extensively studied to fully replace the above propellants, so called green propellant such as ADN(Ammonium dintramide) and HAN(Hydroxylammonium nitrate)

First of all, ADN, which is synthesized in soviet union at first, has yellow needle shaped crystal configuration. The solubility on water is about 78%. A flight test of ADN thruster, shown in Fig. 1.5 developed by ECAPS, Sweden, has been carried out using LMP-103S green monopropellant, of which the ADN, methanol, and water are major components, equipped on PRISMA satellite in

2010. A synthesis of ADN is achieved through the nitro reaction which requires fuming nitric acid and concentrated sulfuric acid to maintain a low acidic environment.

Meanwhile, HAN is initially developed for an liquid gun propellant named XM46(or LMP1846). An unique application of HAN is usage on plutonium reduction agent on nuclear plant. The instability of HAN is reported through various accident reports due to its auto catalytic reaction under iron ion contamination[28]. Nevertheless, considerable works have been conducted to increase the stability. As a result, SHP-163 propellant and AFM-315E are developed in JAXA and NASA, respectively. Theses propellants are equipped on the SDS-4(JAXA) and GPIM(NASA) thruster, and space flight tests of both propellants have conducted since early 2019. Compare to ADN, HAN has difficulties in crystallization due to its moisture absorbance nature. Meanwhile, the solubility is up to 95% which leads to higher density specific impulse. Table 1.2 shows the comparison on N2H4. H2O2, LMP-103S, and AFM-315E. Compare to N2H4, LMP-103s and AFM-315E have 104% and 117% higher specific impulse, respectively. Density specific impulse is more higher than N_2H_4 thruster.

As ADN and HAN based propellants have developed almost simultaneously for space application, some similar problems are reported, ignition. Both propellants have high activation energy. Therefore, ignition is conducted through the catalytic decomposition. According to the recent report, the PRSIMA satellite requires 10min with 6W heater to reach the optimum catalyst bed temperature for LMP-103s ignition[29]. In addition, the author points out that the catalyst pre-heating time prevents immediate response of the thruster system and may have similar obstacles on HAN based propellants. As the novel green propellants ignition problems are surfaced, various methods have been suggested. In Utah state university, they develope ABS(acrylonitrile butadiene styrene) plasma igniter which produces enough high temperature to ignite 24wt% HAN solution via combustion reaction with carbohydrate gas from ABS surface due to plasma heating and additional oxygen gas[30]. The result shows that the igniter has a capability to decompose the 24wt% HAN solution continuously, after turning off

the igniter. Arc plasma employed ignition method is also carried out using HAN/Ethanol blended propellant[31]. The authors conducts the synergetic effects between the propellant injection direction and arc plasma consuming ~20 A / ~120V electric power consumption. Moreover, Khare et al. introduces the electrolytic ignition and gasification of XM46 propellants[32-34]. The controlled parameters are input power and electrode surface area. The ignition delay time is significantly as the input voltage and power are increased. The least ignition delay time is 5 sec applying 320 W. However, the electrode surface effects are rarely significant. The maximum decomposition temperature is around 120 ℃ regardless of the input power.

Among the introduced ignition method, electrolytic decomposition seems to be the most desirable method. Despite of some advantages that ABS igniter and plasma ignition provide sufficient heat energy to initiate the ignition and decomposition of HAN propellant at low concentration, additional oxidizer tank and large power consumption, which makes the thruster system further larger, are inevitable to each method, respectively. However, electrolytic decomposition is worked by two electrodes, and power consumption is relatively lower than plasma and no additional oxidizer tank is required. Therefore, an ignition method in this thesis employs the electrolytic ignition as an alternative way to ignite HAN based monopropellant with low energy consumption.

(a) (b)

Fig. 1.2 (a) 3600N hydrazine based thruster; Rocket dyne, (b) 30N(top) and 200N(bottom) thruster; KARI and HANHWA

Fig. 1.3 Hydrazine handling process (NASA)

FIg. 1.4 Developed H_2O_2 thrusters for KSLV - II RCS

Table 1.2 Summaries on conventional and novel monopropellants

Properties	N_2H_4	H_2O_2	LMP-103s (ADN based)	AFM-315E (HAN based)
I_{sp} (sec)	200 ~ 220	140 ~ 190 (70 ~ 86%)	205 ~ 230 (100 ~ 104%)	231 ~ 257 (117%)
ρI_{sp} (N・s/L)	2000 ~ 2200	1940 ~2640 (97 ~ 120%)	2540 ~ 2850 (130%)	3101 ~ 3450 (155%)
Tad (K)	873	910 (104%)	1891 (216%)	2167 (248%)
LD50 (mg/kg)	60	2000	823	550
Advantages	・Reliability ・Low Tad	・Reliability ・Handling	・Non toxic ・High performance	
Disadvantages	・Toxicity ・Handling	・Low performance ・Compatibility	・Synthesis ・Ignition	・Metal compatibility ・Ignition
Flight test	Proven		Proven (2010)	In- flight (2019)
Accessibility	Limited	Unlimited	Unlimited	Unlimited

1.4 Gel propellant

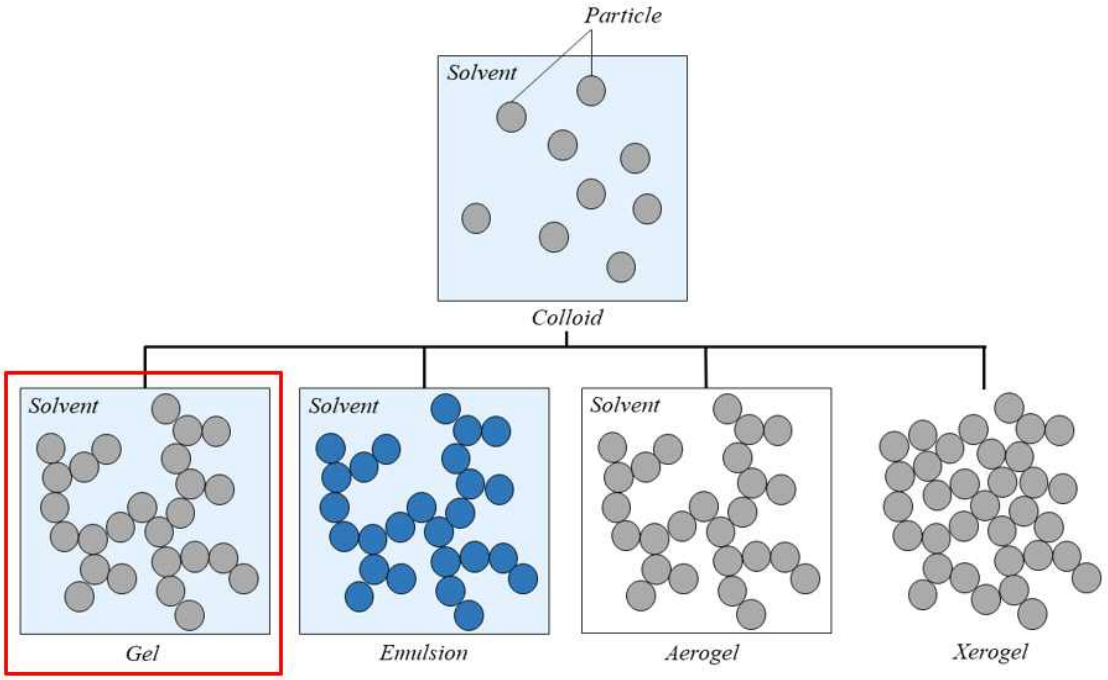

Fig. 1.5 Classification of various solute/solvent mixture

Fig. 1.6 describes the various schematics for solute and solvent mixture. In general, if more than two ingredients are mixed in single volume, it is called mixture or compound. However, when the solute size is few micro to nano scale, the gravitational force acting on the particles becomes smaller than buoyancy force. Therefore, the particles are tend to stay in dispersed rather being precipitated or floated. This state is called colloid that the micro to nano scale particles are well dispersed in a solution. If the some molecular portion of particles are crosslinked with liquid solution and/or crosslinked by a certain agent, the state is called gel. Emulsion and aerogel are made up of liquid state solvent/solute and of gas phase solvent/solute, respectively. Xerogel is that the solution is highly concentrated state. The industrial application on emulsion are cosmetics, such as lotion and cream. Aerogel is used in thermal protection technology due to its high thermal insulation characteristic.

In order to understand the gel propellant further, a distinct property of the propellants is a thixotropic nature shown in Fig. 1.7. Though various kinds of liquid, such as water and alcohol, have a viscosity, it is very small compare to a thixotropic liquid. Because the viscosity is constant at variable shear stress. This types of fluid is called Newtonian fluid, where the relationship between shear rate and shear stress is shown in Eq. 1.1,

$$\tau = \mu \frac{d\gamma}{dt} \qquad \text{Eq.1.1}$$

where the τ, μ, and $d\gamma/dt$ is shear stress(Pa), viscosity(Pa·s), and shear rate(s^{-1}), respectively.

However, if the viscosity is variable with shear rate, the fluid is called non-newtonian and the relationship is shown in Eq. 1.2,

$$\tau = \mu \left(\frac{d\gamma}{dt} \right)^n = \eta \frac{d\gamma}{dt} \qquad \text{Eq.1.2}$$

where the $\eta = \mu \left| \frac{d\gamma}{dt} \right|^{n-1}$ is apparent viscosity(s^{1-n}), and n is found through the experiment. The Non-newtonian fluid is further divided into shear thickening where the $n>1$, and shear thinning where the $n<1$.

The application of gel in space technology have reported since 1970 by Glassman et al.. The authors suggested the gel propellant to disperse the metal fuel or additional component homogeneously[35]. After then, many institutions have carried out extensive study on gel propellant. The advantages on gel propellant are as belows.

1) Decreased vapor pressure and toxicity
2) Capabilities of increased propellant energy contents
3) Decreased fuel sensitivity
4) Avoid the fuel sloshing

As the vapor pressure is decreased, accessibility to toxic propellant becomes easier. Furthermore, the propellant energy content to increase the rocket performance can be achieved by mixing with some energetic thickening agent. In addition, increased viscosity lower the fuel sensitivity so that the unexpected accident is avoidable. Finally, the sloshing phenomenon which may cause the vibrational failure on rocket structure is avoidable. Conventional gel propellants are summarized in Table. 1.3. Hydrazine and its derivatives are extensively studied using various thickening agents. Nitric acid as an oxidizer is also studied as it has hypergolic characteristic with various fuels such as hydrazine. However, little study is introduced using green monopropellants such as ADN, and HAN. The reason is expected to be that the green propellants for space application is relatively novel one. The anticipated benefits of gelled green monopropellants are decreased propellants sensitivity and increased density impulse. Therefore, the HAN which is high accessibility from synthesis to analysis is chosen as oxidizer of gelled green monopropellants in this study.

The research scope and aim of the thesis is from synthesis to ignition of the green gelled monopropellant. HAN is chosen as major component which performs as an oxidizer of the gelled propellants. As mentioned earlier, the ignition characteristic of HAN monpropellant using thermal and catalytic decomposition has a few problems. Therefore, the electrolytic ignition is employed in this paper. Furthermore, gelling process is carried out using cellulose derivatives which are commonly used in other propellants. In this thesis, the synthesis of HAN and its analysis is carried out using various analysis technique. In addition, the gelled propellant is analyzed. The electrolytic ignition characteristic is evaluated in various perspective.

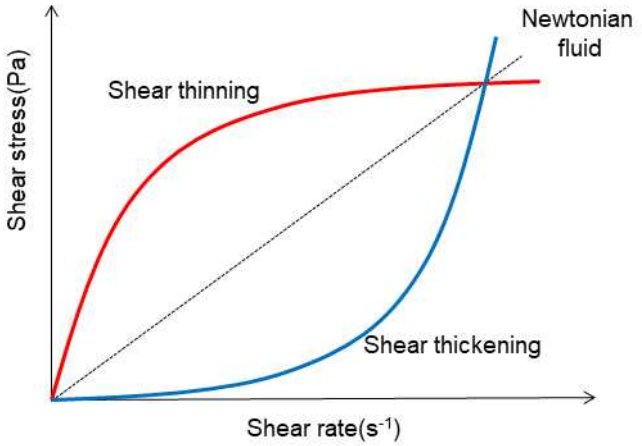

Fig. 1.6 Schematics of Newtonian and non-newtonian fluid

Table 1.3 Gelling agent and its combination with propellants[36,37]

Propellant		Gelling agent	Additive
Fuel	Hydrazine UDMH MMH	SiO2 Carbopol aerosil	Aluminum
	RP-1 JP-10 Keroene	SiO2 Cellulose and its derivatives Propylene glycol	
Oxidizer	RFNA/WFNA	SiO2	
	H_2O_2	PVP, Agarose	Boron
Mono propellant	ADN/HAN/HNF	N/A	N/A

Chapter 2. Experiment and discussion

2.1 Material preparation

HAN can be synthesized by catalytic reaction, ion exhange, electrolysis, hydrogenation of nitric acid, double decomposition, and neutralization method. Though there are various methods, the double decomposition and neutralization methods are widely employed for laboratory uses. HAN preparation using double decomposition method is achieved with hydroxylammonium sulphate($(NH_3OH)_2 \cdot H_2SO_4$) and metal nitrate($M(NO_3)_2$), shown in (R.a)

$$(NH_2OH)_2 \bullet H_2SO_4 + M(NO_3)_2 \rightarrow 2NH_3OH^+ \bullet NO_3^- + MSO_4 \quad \text{(a)}$$

M is a transient metal, such as Barium and Calcium

However, the final product may contain the transient metal ions such as barium or calcium when employing double decomposition method. The existence of metal ions in HAN solution may cause the auto-catalytic reaction, shown in (R.1) to (R.3).

$$2NH_3OH^+ + 4Fe^{3+} \rightarrow 4Fe^{2+} + N_2O + H_2O + 6H^+ \quad \text{(R.1)}$$

$$2Fe^{2+} + HNO_3 + 2H^+ \rightarrow 2Fe^{3+} + HNO_2 + H_2O \quad \text{(R.2)}$$

$$HAN + HNO_2 \rightarrow N_2O + 2H_2O + HNO_3 \quad \text{(R.3)}$$

For example, when iron(Fe) ions are contained in the solution, hydroxylammonium ions reduce the trivalent iron ions(Fe^{3+}) to divalent iron ions(Fe^{2-}) and produce the hydrogen protons(H^+) that reacts with the nitrate ions(NO_3^-) to produce the HNO_3. The production of nitric acid via hydrogen proton transfer reaction is known as initial step of HAN decomposition. Furthermore, HNO_3 oxidize the Fe^{2+} to Fe^{3+} with producing nitrous acid(HNO_2).

In the previous research, HNO_2 causes the additional decomposition of HAN with producing the HNO_3. As a result, (R.1) to (R.3) is proceeded, repeatedly. Therefore, any metal ions in HAN solution must be eliminated. As shown in above reaction (R.a), double decomposition method involves additional steps to eliminate any metal ions.

Meanwhile, HAN preparation by neutralization method is achieved using hydroxlamine(NH_2OH) and nitric acid(HNO_3), shown in (R.b).

$$NH_2OH + HNO_3 \rightarrow NH_3OH^+ + NO_3^- \quad \text{(b)}$$

Theoretically, all satrting materials are essentially metal free. Hence, metal elimination steps are not required. However, the cooling system should be equiped in order to prevent unexpected HAN decomposition during the synthesis process as the temperature is increased as a result of neutralization reaction. In this research, the neutralization method is employed to prepare HAN solution using 50wt% NH_2OH solution(Alfa aesar, USA) and 70wt% nitric acid(SAMCHUN, South Korea), as received. A theoretical HAN content with above materials is 61.53 wt%. There are two empirical formulas for HAN density to identify the concentration, suggested by the Balistic Research Laboratory and Courthéox et al., shown in Eq. 2.1 and Eq. 2.2, respectively[38,39].

$$\rho_{HAN} = 0.9935 + 0.0463M - 0.0004007M^2 \ (\dagger T = 20℃) \quad \text{Eq.2.1}$$

$$\rho_{HAN} = \frac{107.85}{96.042 - wt\%_{HAN} \times 30.99} \ (\dagger T = 25℃) \quad \text{Eq.2.2}$$

M in Eq. 1 indicates molarity which indicates the number of moles of the solute per 1L solution. The translation from M to wt% is calculated using Eq. 2.3. An obtained HAN solution using neutralization method is 59wt%. For further concentration, the solution is placed in the vacuum chamber under 10^{-2} Torr and 40 ℃ with a desiccant for 16 hours. After the vacuum process, the density of final

$$wt\%_{HAN} = \frac{M \cdot MW}{M \cdot MW + 1000 - (\frac{M \cdot MW}{1.84}) \times 100} \quad \text{Eq.2.3}$$

final product is remeasured using Eq. 1 and Eq. 2. As a result, a highly concentrated HAN solution(~95wt%) and crystallized HAN are obtained. In order to verify that the product is HAN, FT-IR(Fourier transform-infrared) and laser raman spectroscopy are carried out. AN(ammonium nitrate), which has similar chemical structure to HAN structure, is used as a comparative sample. In addition, the TGA(Thermogravimetric analysis) is carried out using the SHP 163 propellant of which the HAN, AN, methanol, and water are the major components with 95:5:8:21 mass ratio, respectively. All analyzed results is compared with previous research results[40-42].

The chemical structures of AN and HAN are shown in Fig. 2.1. Both substances have NO_3^- anion. However, the distinct difference is represented in cation structures. Compare to cation structure of AN, HAN has N-OH and O-H bonding structure. This difference is shown in laser raman and FT-IR spectroscopy.

The laser raman spectroscopy result is shown in Fig. 2.2. Unlike the AN peak spectrum, HAN has distinct peak spectrum around 1010cm^{-1} range because of N-OH stretch structure which is not shown in AN spectrum. Other spectrums for HAN are shown in 730, 1050, and 1420 cm^{-1} for NO_3, 1050 cm^{-1} for N-OH, 1190 cm^{-1} for O-H, and 1620 cm^{-1} for NH_3.

The FT-IR results of highly concentrated solution state and crystal state of HAN is shown in Fig. 2.3. The spectrums of 830, 1050, and 1300 cm^{-1} for NO_3, 1179, 1510, 2720, and 2950 cm^{-1} for NH_3, and 3150cm^{-1} for O-H are shown, and more sharp peak spectrums are shown in crystal state and from 2500 to 3300 cm^{-1} range.

The TGA result for SHP 163 is shown in Fig. 2.4. The slight decomposition is started around 50 ℃. The major decomposition process is occurred in 196 ℃ and 212 ℃ which are due to the water vaporization and methanol decomposition, respectively. Throughout the spectroscopy analysis and TGA results, the HAN is synthesized and confirmed.

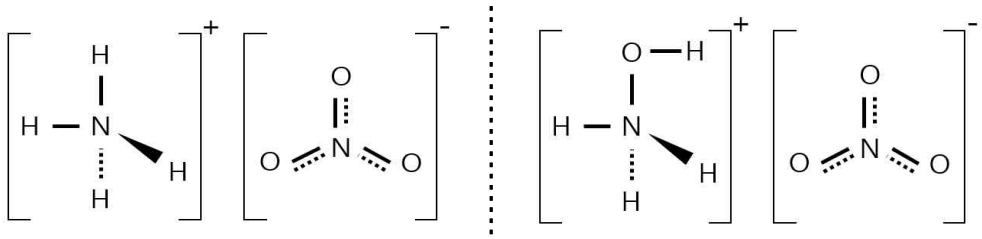

Fig. 2.1 Chemical structure of AN(Left) and HAN(Right)

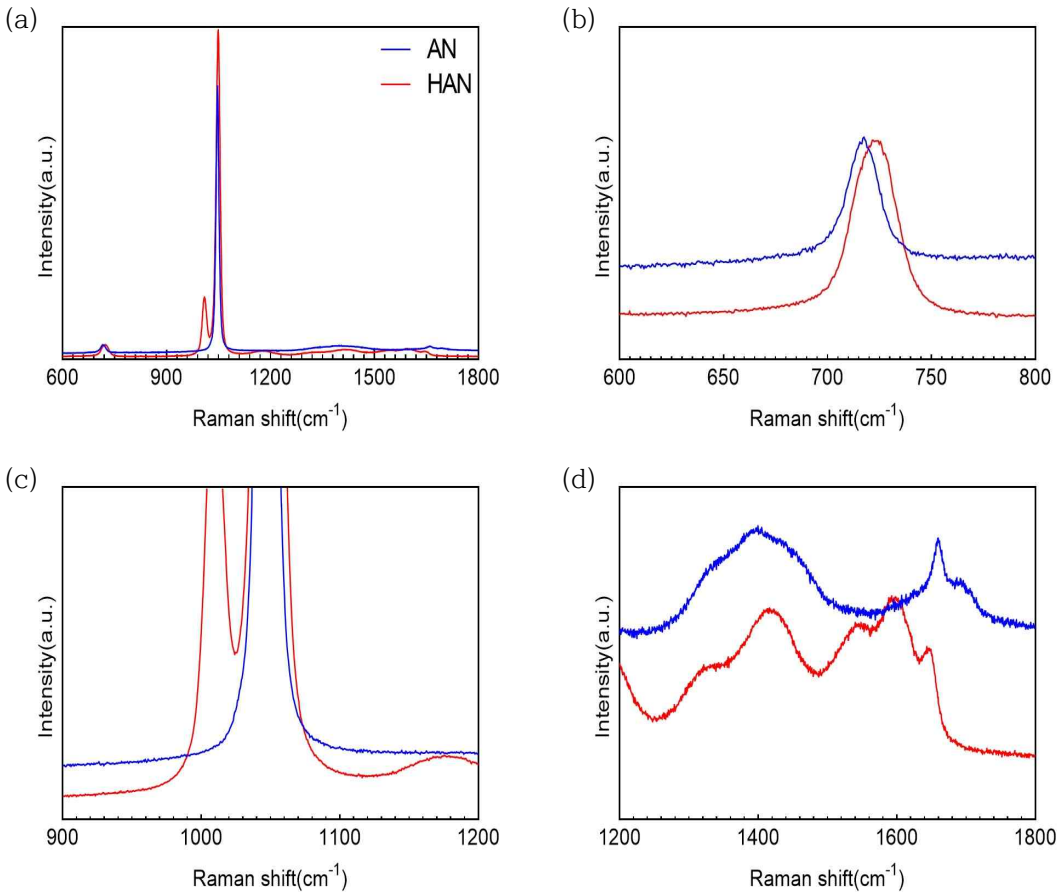

Fig. 2.2 Laser raman spectrum for AN(Ammonium nitrate) and HAN; (a) Full Laser raman spectrum for AN and HAN, (b) NO3 : 730cm−1, (c)N−OH stretch : 1010cm−1, NO3 : 1050cm−1, O−H stretch : 1190cm−1, (d) NO3 : 1420cm−1, NH3 : 1620cm−1

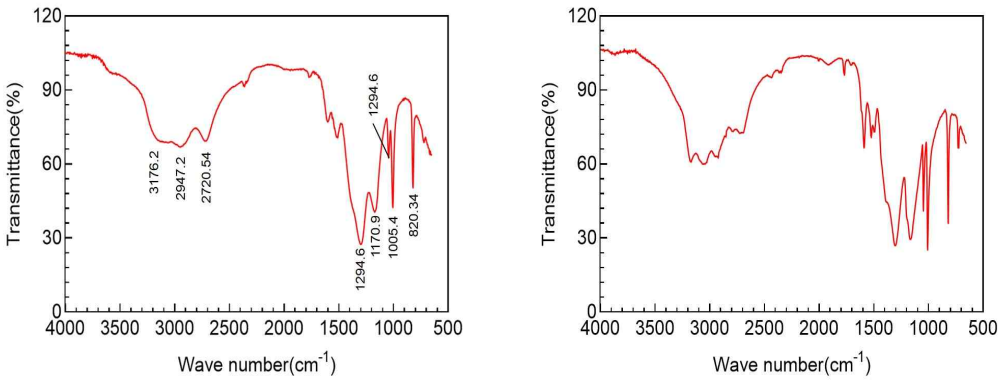

Fig. 2.3 FT-IR spectrum for HAN(solution for left, solid for right); NO3 : 830, 1050, 1300cm-1, O-H stretch : 3150cm-1, NH3 : 1179, 1510, 2720, 2950cm-1

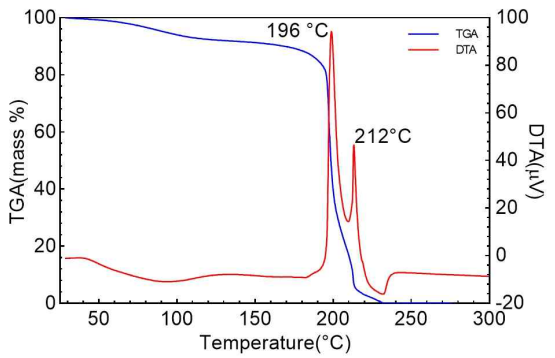

Fig. 2.4 TGA and DTA result of SHP 163 with 5℃/min in nitrogen atmosphere

2.2 Gelation and analysis of HAN

The gelation process for HAN monopropellant is carried out. The Hydroxyl-Propyl Methyl Cellulose(HPMC) is chosen as a thickening agent. The solvent is SHP 163. If HAN is used solely, some liquid is spilled during the storage. The expected reason is due to compatibility between HAN and HPMC. Therefore, as the HPMC contains methyl component, SHP 163, which contains methanol, is chosen as a solvent. As a result, compatibility is resolved. The theoretical rocket performance is calculated using NASA CEA code, shown in Fig. 2.5. The 0 wt% of cellulose means the pure SHP 163 of which the vacuum specific impulse($I_{sp,vac}$, sec) and adiabatic flame temperature(T_{ad}, K) is about 273, and 2400, respectively. As the cellulose content is increased, the performance is slightly decreased, except for 1 wt% of which the $I_{sp,vac}$ and T_{ad} are 274 and 2420, respectively. In this research, the cellulose content is 5 wt% because of mixing process. In order to sustain proper viscosity, the agent content must exceed at least 4 wt% which is examined experimentally. However, if the agent content exceeds over 8 wt%, the viscosity is extremely increased so that the propellant agglomerates by itself during the mixing process. The result for 30 and 40 wt% cellulose are shown in Fig. 2.6. For this reason, the agent content is 5 wt% and the result is shown in Fig. 2.7.

The TGA is also carried out for 5 and 10 wt%, shown in Fig. 2.8. Compared to Fig. 2.4, The reaction is one-step reaction. In addition, the major decomposition is occurred at 130 and 147 ℃ for 5 and 10 wt%, respectively. Through the TGA result, the thermal stability is lower than pure SHP 163. The reason is due to the carbon content is increased compare to HAN solution. However, lower decomposition temperature would be lower the required on set temperature, furthermore, the lower thermal sensitivity can be resolved by adding other stabilizers.

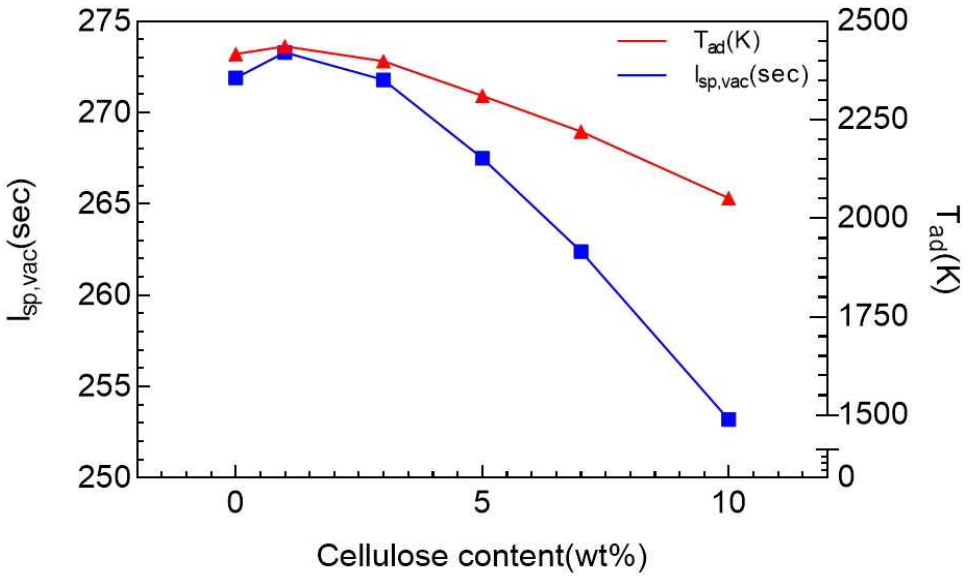

Fig. 2.5 Characteristic of adiabatic temperature and specific impulse with cellulose content change

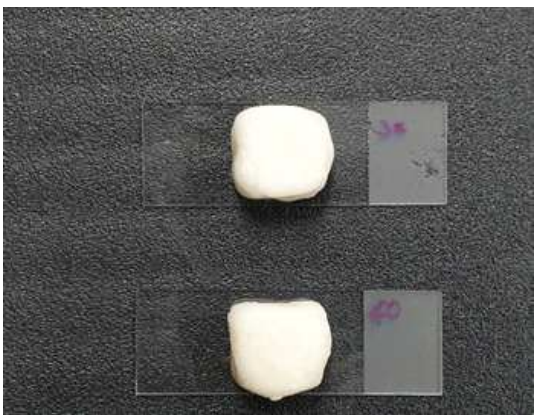

Fig. 2.6 Gelled propellants with 30 and 40 wt% HPMC contents

Fig. 2.7 Gelled propellants with 5 wt% HPMC contents

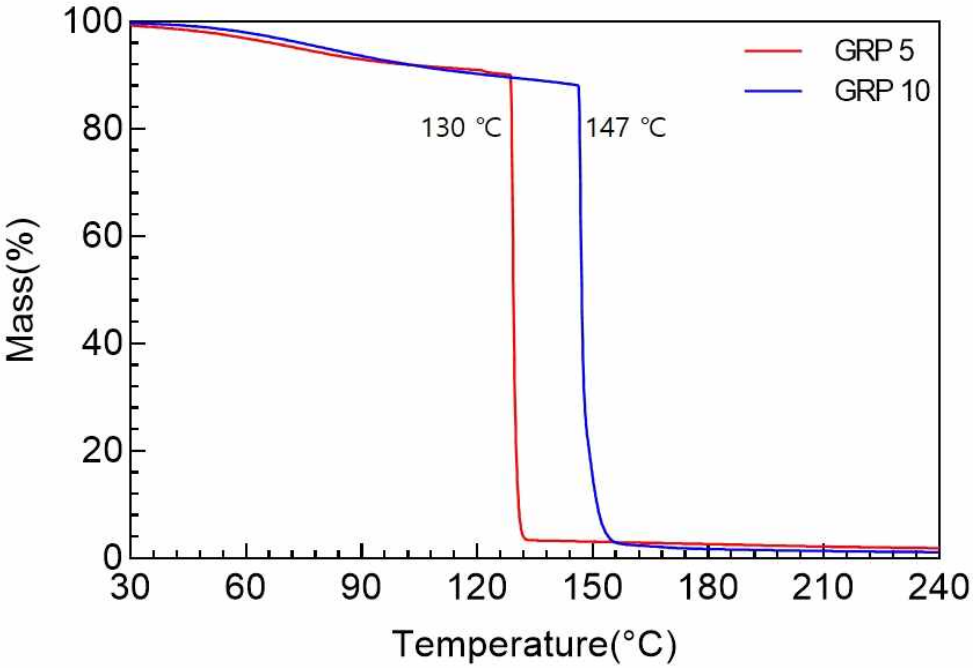

Fig. 2.8 TGA and DTA profile of gelled HAN propellant with 5 ℃/min in nitrogen atmosphere

2.3 Experiment set-up

The experiment set-up for electrolytic ignition of gelled HAN propellant is shown in Fig. 2.9. The 15g of propellant is stored into the ∅30, 80 mm height quartz tube. The electrode dimension and material are ∅4 and copper, respectively. In addition, two types of copper electrode are used, rod type and foam type. All electrode is immersed into the propellant. The immersed depth and distance between anode and cathode side electrodes are about 12 mm and 20 mm, respectively. In order to supply enough electric power, high voltage power supply is used which reports the voltage and current data simultaneously. Furthermore, the electric circuit is connected to the NI DAQ(Data AQuisition) to distinguish the ignition delay time between power input time and ignition time. Finally, the K-type thermocouple is placed 10 mm above the propellant surface to define the ignition point by temperature increase. The voltage and current data are acquired through HVPS control software program, and temperature data is acquired through the NI-DAQ system. The input voltage is varied from 12 to 48 VDC for rod type and 48 VDC only for foam type. The current is limited to 3 A.

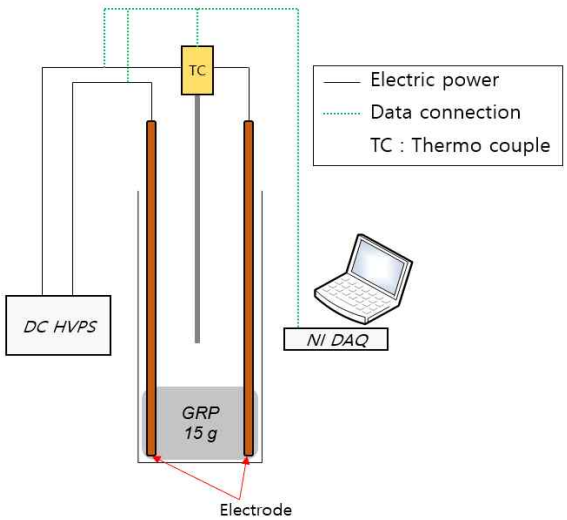

Fig. 2.9 Experimental set-up for electrolytic ignition of gelled HAN propellant

2.3 Result and discussion

Experiment results for 12, 24 V and 48 V using rod type electrode are shown in Fig. 2.10 and Fig. 2.11, respectively. When applying 12 V at t= 5 sec in Fig. 2.9, the sharp current peak is observed due to the mechanical characteristic of HVPS. Average power is 12 W with 1 A current. The temperature is slightly increased after applying the power. The temperature increasement slope from 5 sec to 170 sec is 1.8 ℃/min, and from 170 to 340 sec is 12 ℃/min. After 340 sec, rapid increasement in temperature and power is observed due to the propellant decomposition which occurred when the peak power is reached. After the decomposition is initiated, the current flow is stopped due to decrease of ionic substances, for instance, NH_3OH^+ or NO_3^-. The maximum temperature when applying 12 V is 242 ℃.

In the case of 24 V input, the maximum current flow is 1.6 A. The initial operation characteristic is similar with 12 V experiment. The ignition delay time for 12 V is 25 sec, The maximum power and temperature in this test are 42 W and 183 ℃, respectively.

In the case of 48 V input, the HVPS operation mode is changed from constant voltage mode to constant current mode. Hence, the maximum voltage is around 31 ~ 38 V, and the current is limited to 3 A. The ignition delay time is 4 sec which is the shortest among the tests. The maximum power and temperature are 114 W and 192 ℃, respectively.

The combustion behaviors are same in all cases. The initial reaction is occurred at the anode side. In Fig. 2.12 which represents the combustion behavior with 24 V test, #1 shows when electric power is applied. In addition, the bubbles, which is the hydrogen gases, are formed in both anode and cathode side because of the electrolytic reaction, shown in table 2.1, (R.2.1) to (R.2.4). Furthermore, the blue colored substances are formed which is copper nitrate($Cu(NO_3)_2$). #2 shows the decomposition point and the substantial gases are generated at the anode side. This gas is expected to be the water vapor. The overall reaction is shown in #3. The brown gas is expected to be the NO_2 gas. The combustion result using rod type electrode is very similar with HAN solution thermal decomposition.

However, when using the foam type electrode, the result is different compared to test results using rod type electrode. The result is shown in Fig. 2.13. The maximum power is 59 W with 48 V and 1.3 A. Especially, the current is kept constantly, rather the voltage is increased from 15 V to 48 V. The ignition delay time is 20 sec and the maximum temperature is reached to 748 ℃ with fully developed combustion and luminous flame. A formation of $Cu(NO_3)_2$ is also observed at the anode side. Furthermore, the decomposition is initiated as the gas is exhausted at the cathode side unlike when using rod type electrode.

As shown in above test results, the major parameter that reduces the ignition delay time is electric power. For example, when using the rod type electrode with 12 V input, the resistance of the propellant is increased to 120 sec that can be deduced through ohm's law and relationship between voltage and electric power. The reason why the resistance is increased is that the NO_3^- ions react with copper. Therefore, the ions that makes the current to flow across the propellant are decreased, resulting the decrease of current. However after the 120 sec to 320 sec, the power is increased again which means that the resistance is decreased and the ions are increased. The reaction at this region is due to a decomposition reaction of HNO_3 in (R.2.3.1)to (R.2.3.3)

$$HNO_3 \rightarrow NO_2^+ + OH^- \quad \text{(R.2.3.1)}$$

$$NH_2OH + NO_2^+ \rightarrow H_2NO^+ + HNO_2 \quad \text{(R.2.3.2)}$$

$$H_2NO^+ + OH^- \rightarrow H_2O + HNO \quad \text{(R.2.3.3)}$$

The formation of nitrogen dioxide ion(NO_2^+) and hydroxide ion(OH^-) decreases the resistance that allows more current to flow. The above lumped reaction with NH_2OH is (R.2.5). Furthermore, the formation of HNO and HNO_2 accelerates the decomposition of HAN which leads to thermal decomposition behavior. The assumption is concluded in Fig. 2.11. Initial decomposition and HNO_3 decomposition is accelerated by the higher electric power so that decreases the ignition delay time by generating HNO_2 and HNO pool more rapidly.

In the case of using foam type electrode, more complex reaction is expected that the metal component, copper, is involved in the reaction. As the copper is one of the transient metals, contamination by the copper becomes HAN more unstable. As the foam has lower structural modulus, some portion of the electrode is easily detached. Therefore the electrode involves as a fuel leading to overall combustion. In this case, no substances are left except for small amount of soot formation inside the tube. The energy consumption and other results in this experiments are summarized in table 2.2.

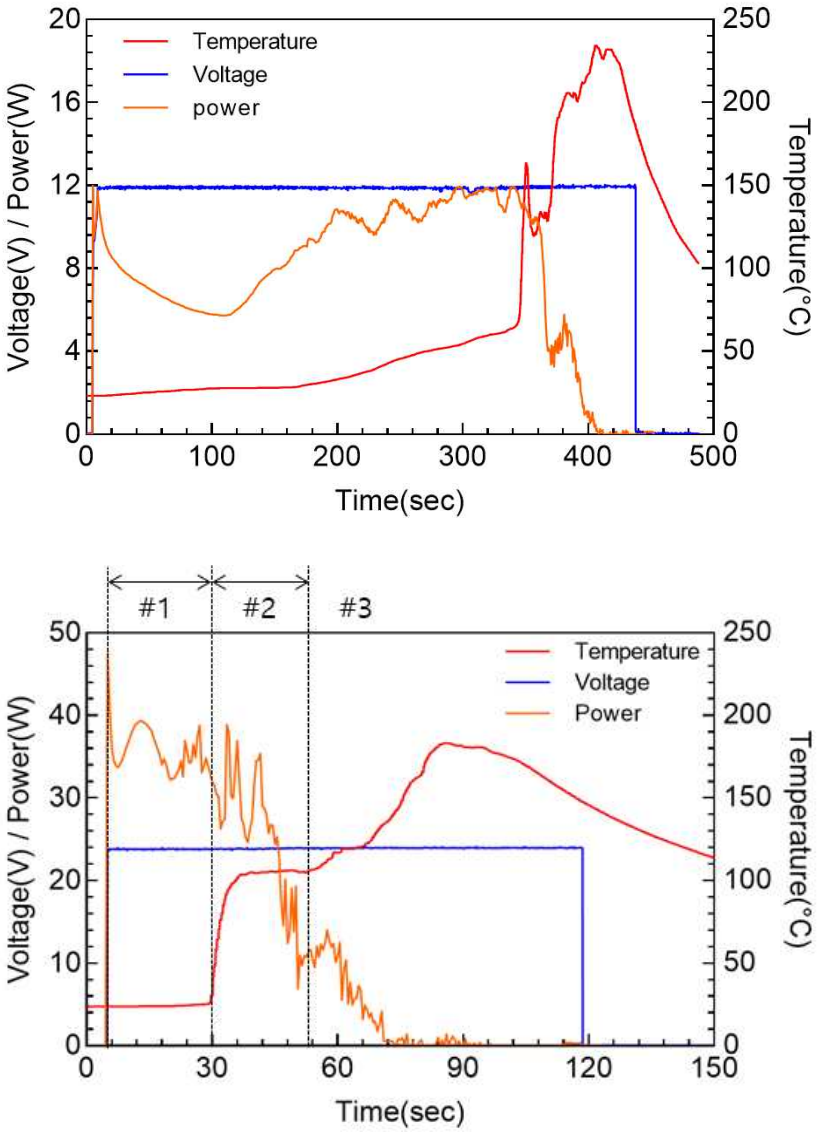

Fig. 2.10 Electrolytic ignition of gelled HAN propellant for 12V(Top), 24V(Bottom) with copper rod

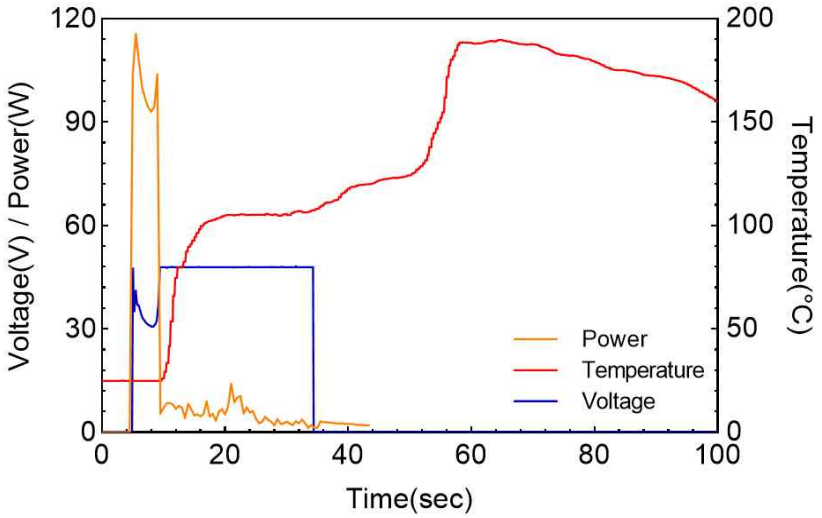

Fig. 2.11 Electrolytic ignition of gelled HAN propellant for 48V with copper rod

#1 #2 #3

Fig. 2.12 Representative behavior of gelled HAN propellant electrolytic ignition with 24V; #1 : Initial reaction with electrode, #2 : Initiation of ignition, #3 : Ignition without power input; Left side electrode is cathode(−), right side electrode is anode(+)

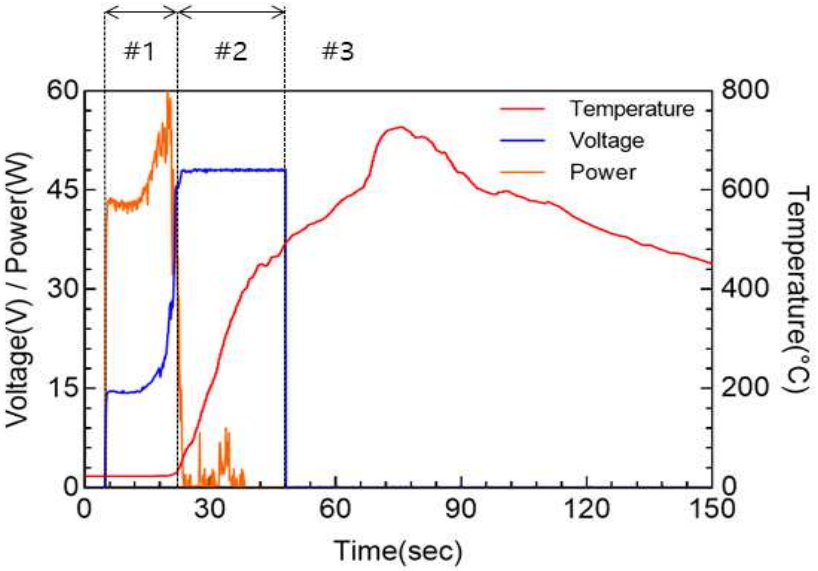

Fig. 2.13 Electrolytic ignition of gelled HAN propellant for 48V with copper foam

#1 #2 #3

Fig. 2.14 Behavior of gelled HAN propellant electrolytic ignition with copper foam; #1 : Initial reaction with electrode, #2 : Initiation of ignition, #3 : Ignition without power input; Left side electrode is cathode(+), right side electrode is anode(−)

Table 2.1. Electrolytic ignition pathways for Gelled HAN propellant

Electrolytic initiation	
$H_2O \rightarrow 2H^+ + 0.5O_2 + 2e$	(R2.1)
At cathode	
$NO_3^- + H^+ \rightarrow HNO_3$	(R.2.2)
$2HNO_3 + Cu \rightarrow Cu(NO_3)_2 + H_2$	(R.2.3)
At anode	
$2NH_3OH^+ + 2e^- \rightarrow 2NH_2OH + H_2$	(R.2.4)
HAN overall reaction	
$HNO_3 + NH_2OH \rightarrow HONO + HNO + H_2O$	(R2.5)
$NH_2OH + HNO_2 \rightarrow N_2O + 2H_2O$	(R2.6)
$NH_2OH + HNO \rightarrow N_2 + 2H_2O$	(R2.7)
$3HNO_2 \rightarrow 2NO + HNO_3 + H_2O$	(R2.8)
$2HNO \rightarrow N_2O + H_2O$	(R2.9)
$HNO + HNO_3 \rightarrow 2HNO_2$	(R2.10)
$HNO_2 + HNO_3 \rightarrow 2NO_2 + H_2O$	(R2.11)

Table 2.2. Summary on experiment result; CV : constant voltage, CC: constant current

Item \ Set voltage	12 V	24 V	48 V	
Input voltage (V)	12 (CV)	24 (CV)	48 (CV)	15 ~ 48 (CC to CV)
Igntion delay time (sec)	352	25	4	25
T_{max}(℃)	242	183	192	748
P_{peak}(W)	12	42	114	59
Pavg(W)	9.4	37.3	101.2	48.4
E_{cons}(J)	3308.8	932.5	404.8	1210

Chapter 3. Conclusion

An experiment study on electrolytic ignition of gelled green monopropellant using HAN and HPMC is carried out in this paper. The green propellant, HAN, that replaces the conventional toxic propellants such as hydrazine and hydrogen peroxide is synthesized in laboratory scale. The verification process is also carried out using laser raman and FT-IR spectroscopy. As a result, each peak values are compared with previous research. One major distinct characteristic of chemical structure of HAN is shown in both results by comparing with the AN spectrum. Moreover, TGA is carried out using SHP 163 monopropellant. The thermal decomposition is observed around 196 ℃ and 210 ℃ which indicates the water evaporation and methanol reaction, respectively. In addition, HAN based green gelled propellant is synthesized using HPMC. The HPMC content is controlled by 5 wt% considering the mixing process. TGA result showed that the decomposition temperature is decreased to 130 ℃ and single step reaction is observed. The electrolytic ignition test of the gelled HAN propellant is carried out using copper based rod and foam type electrode. The power consumption is from 12 W to 114 W. Energy consuption is varied from 400 J to 3300 J. Compared to the report that describes an igntion characteristic of LMP-103S which consumes about 3,600 J to preheat the catalyst bed, 11.1 % energy is consumed to initiate the propellant decomposition. The ignition characteristic of the propellant is as same as thermal decomposition behavior. In addition, the ignition delay time is substantially decreased up to 5 sec. Moreover, when using foam type electrode, the produced energy is considerably increased as the detached metal particle involves the reaction. In this study, various ignition characteristics are evaluated. With further experiments and proper electrode selection considering mission time, the application of HAN based gelled propellant would be the best option for green environment, and satellite mission efficiency.

Reference

1. Sutton, G.P., and Biblarz, O., "Rocket propulsion elements", WILEY

2. Negri, M.,Wilhem, M., Hendrich., C., Winnborg, N., Gediminas, L., Adelöw, L., Maleix, C., Chabernaus, R., Brahmi, R., Beauchet, R., Batonneau, Y., Kappenstein, C., Koopmanse, R.J., Schuh, S., Bartok, T., Scharlemann, C., Gotzig, U., and Schwentenweing, M., "New technologies for ammonium dinitramide based monopropellant thrusters – The project RHEFORM", Acta Astronautica, Vol. 143, pp.105-117, 2018

3. Rachuk, V., and Titkov, N., "The first Russian LOX-LH2 Expander cycle LRE: RD0146", 42nd AIAA/ASME/SAE/ASEE Joint Porpulsion Conference and Exhibit, AIAA 2006-4904, C.A., U.S.A., 2006

4. Lee., S.H., Jo., S.H., Kim., S.R., and Lee., S.J., "A Numerical Study on the Simulation of Power-pack Start-up of a Staged Combustion Cycle Engine"., Journal of the Korean Scoiety of Propulsion Enginners, Vol. 23, No. 3., pp. 58-66, 2019

5. Kim., C.H., Lee., J.H., Woo., S.P., So., Y.S., Lee., S.J., Lee., K.J., Jo., N.K., Han., Y.M., and Kim., J.H., " Development Status of Technology Demonstration Model for Staged Combustion Cycle Engine", Journal of the Korean Scoiety of Propulsion Enginners, Vol. 23, No. 4., pp. 104-111, 2019

6. Inatani., Y., Nauro, Y., and Yonemoto, K., "Concept and Preliminary Flight Testing of a Fully Reusable Rocket Vehicle", Journal of Spaccraft and Rockets, Vol. 38, No. 1, pp. 36-42, 2012

7. John., J., Nandagopalan., P., Baek., S.W., and Cho., S.J., "Hypergolic ignition delay studies of solidified ethanol fuel with hydrogen peroxide for hybrid rockets", Combustion and flame, Vol. 212, pp.205-215, 2020

8. Baier., M.J., Ramachandran., P.V., and Son., S.F., "Characterization of the hypergolic ignition delay of ammonia borane", Journal of Propulsion and Power, Vol. 35, No. 1, pp.182-189, 2018

9 Pourpoin, T.L., and Anderson, W.E., "Environmental Effects on Hypergolic Ignition", 41st AIAA/ASME/SAE/ASEE Joint Propulsion Conference & Exhibit, AIAA 2005-3581, A.Z., July, 2005

10. Kang, H.J., Jang, D.W., and Kwon, S.J., "Demonstration of 500N scale bipropellant thruster using non-toxic hypergolic fuel and hydrogen peroxide", Aerospace and Science Technology, Vol. 49, pp.209-214, 2016

11. Spores, R.A., Masse, R., Kimbrel, S., and McLean, C., "GPIM AF-M315E Propulsion System", 49th AIAA/ASME/SAE/ASEE Joint Propulsion Conference & Exhibit, AIAA 2013-3849, C.A., U.S.A., 2013

12. Venkatachalam, S., Santhosh, G. and Ninan, K.N., "An Overview on the Synthetic Routes and Properties of Ammonium Dinitramide (ADN) and Other Dinitramide Salts," Propellants, Explosives, Pyrotechnics, Vol. 29, No. 3, pp. 178-187, 2004

13 Kumar, P., "An overview on properties, thermal decomposition, and combustion behavior of ADN and ADN based solid propellants", Defense technology, Vol.14, No.6, pp. 661-673, 2018

14. Vosen, S. R., "The Burning Rate of Hydroxylammonium Nitrate-Based Liquid Propellants," Proceedings of the 22nd Symposium on Combustion, PA, U.S.A., 1988

15. Lee, Y.J., and Litzinger, T.A., "Combustion chemistry of HAN, TEAN, and XM46", Comustion science and technology, Vol. 141, No.1-6, pp. 19-36, 2007

16. Yim, Y.J., Lee. J.S., Park, E.Y., Choi, S.H., Yoo, J.C., and Cho, Y., "The Study on Minimum Smoke Propellant to Reduce Afterburning Reaction", Journal of the Korean Society of Propulsion Engineers, Vol. 17, No. 5., pp.10-17, 2013

17. Abd-Elghany, M., Klpatötke, T.M., and Elbeih, A., "Environmentally safe (chlorine-free): new green propellant formulation based on 2,2,2-trinitroethyl-formate and HTPB", RSC advances, Issue. 21, pp. 11771-11777, 2018

18. Abd-Elghany, M., Klpatötke, T.M., and Elbeih, "New green and thermally stable solid propellant formulations based on TNEF", International Journal of Energetic Materials and Chemical Propulsion, Vol. 17, Issue. 4, pp.349-357, 2018

19. Sawka, W., and McPherson, M., "A safe, Micro to Macro Propulsion technology", Join propulsion conference, AIAA 2013-4168, 2013

20. Kim, K.M., and Kim, I.C., "The Characteristics and its Development Trends of Thermoplastic Propellants", Journal of the Korean society of propulsion Engineers, Vol. 15, No.3, pp.47-57, 2011
21. Jeong, J.Y., Song, J.K., Kim, Y.G., and Lee, B.G., "Study on the Formulation of an Energetic Thermoplastic Propellant(I)", Journal of the Korean Sociey of Propulsion Engineers, Vol. 23, No. 1, pp. 71-78, 2019
22. Kim, M.J., and Kim, T.G., "Experimental Study of N2O Plasma Igniter for PMMA Combustion", Journal of the Korean Society of Propulsion Engineers, Vol. 23, No. 3., pp. 1-8, 2019
23. Walker, S.D., "High regression rate hybrid rocket fuel grains with helical port structures", Master Thesis, Utah state university, 2015
24. https://www.rocket.com/space/space-power-propulsion/monopropellant-rocket-engines
25. Han, C.Y., Kim, S.K., Won, S.H., and Chae, J.W., "Monopropellant thrusters for a satellite", Current Industrial and Technology Trends in Aerospace, Vol. 11, No. 2., pp. 119-126, 2013
26. Oh, S.K., Kang, S.J., and Oh, D.H., "Hydrogen peroxide monopropellant thruster for KSLV-II reaction control system", Journal of the Korean Society for Aeronautical and Space Science, Vol. 47, No. 5, pp. 353-343, 2019
27. Larson, A., and Wingborg, N., "Green propellants based on Ammonium dinitramide(ADN)", Advances in Spacecraft Technology, Intech.
28. "Technical report on Hydroxylamine nitrate", U.S. Department of energy, DOE/EH-0555, 1998
29. Whitmore, S.A., Merkley, D.P., Eilers, S.D., and Judson, M.I., "Development and Testing of a Green Monopropellant Ignition System", 49th AIAA/ASME/SAE/ASEE Joint Propulsion Conference and Exhibit, C.A., U.S.A., 2013
30. Whitmore, S.A., Merkley, D.P., Eilers, S.D., Judson, M.I., and Taylor, T.L., "Hydrocarbon-Seeded Ignition System for Small Spacecraft Thrusters Using Ionic Liquid Propellants", 27th Annual AIAA/USU Conference on Small Satellite, SSC13-VII-6

31. Wada, A., Watanabe, H., and Takegahara, H., "Combustion Characteristics of a Hydroxylammonium-NitrateBased Monopropellant Thruster with Discharge Plasma System", Journal of propulsio and power, Vol.34, No.4, pp. 1052-1060, 2018

32. Risha, G.A., Yetter, R.A., and Yang, V., "Electrolytic-induced decomposition and igntion of HAN-based liquid monopropellants", International journal of energetic materials and chemical propulsion, Vol. 6, No. 5, pp. 575-588, 2007

33. Khare, P., Yang, V., Meng, H., Risha, G.A., and Yetter, R.A., "Thermal and Electrolytic Decomposition and Ignition of HAN - Water Solutions", Combustio science and technology, Vol.18, No.7, pp. 1065-1078, 2014

34. Meng. H., Khare, P., Risha, G.A., Yetter, R., and Yang, V., "Decomposition and Ignition of HAN-Based Monopropellants by Electrolysis", 47th AIAA Aerospace Sciences Meeting Including The New Horizons Forum and Aerospace Exposition, FL, U.S.A., AIAA 2009-451, 2009

35. Glassman, I., and Sawyer, R.F., "The Performance of Chemical Propellants," Technivision Services, Slough, England, 1970.

36. Aggarwal, R., Patel, I.K., Sharma, P.B., and Thirumalvalavan, "A comprehensive study on gelled propellants", International Journal of Research in Enginnering and Technology, Vol.4, Issue. 9, pp. 286-290, 2015

37. Naumann, K.W., Tussiwand, G., Pinto, P.C., Hopfe, N., Eiender, L., Risse, S., Thumann, A., Niedermaier, H., and Kurth, G., "Green gelled propellant gas generator for high-performance divert and attitude control system", 52nd AIAA/SAE/ASEE Joint Propulsion Conference, AIAA 2016-4667U.T., U.S.A., 2016

38. Sasse, R.A., Davies, M.A., Fifer, R.A., Decker, M.M., and Kotlar, A.J., "Density of Hydroxylammonium nitrate solution", Ballistic Research Laboratory, DTIC, 1988

39. Courthéox, L., Amariei, D., Rossignol, S., and Kappenstein, C., "Thermal and catalytic decomposition of HNF and HAN liquid ionic as propellants", Applied catalysis B : Envrionmental, Vol. 62, pp. 217-225, 2006

40. Van Dijk, C.A., "Characterization of hydroxylammonium nitrate(HAN) at various pressure and temperature", GC-TR-83-266, 1983

41. Hoyani, S., Patel, R., Oommen, C., and Rajeev, R., "Thermal stability of hydroxylammonium nitrate(HAN)", Journal of thermo analysis and calorimetriy, Vol. 129, No.2, pp.1083-1093, 2017

42. Amrousse, R., Katsumi, T., Azuma, N., and Hori, K., "Hydroxylammonium nitrate(HAN)-based, green propellant as alternativs energy resources for potential hydrazaine substitution : From lab ro pilot plant scale-up", Combustion and flame, Vol.176, pp. 334-348, 2017